

Received November 18, 2017, accepted February 17, 2018, date of publication February 21, 2018, date of current version March 28, 2018.

Digital Object Identifier 10.1109/ACCESS.2018.2808338

Full-Duplex Relaying With Quantize-Map-and-Forward

DONG LI¹, (Member, IEEE)

Faculty of Information Technology, Macau University of Science and Technology, Macau 999078

e-mail: dli@must.edu.mo

This work was supported in part by the Macau Science and Technology Development Fund under Grant 052/2016/A and in part by the Faculty Research Grants of the Macau University of Science and Technology under Grant FRG-17-005-FI.

ABSTRACT The quantize-map-and-forward (QMF) has been recently proved to achieve the capacity of arbitrary networks within a bounded gap and optimal diversity-multiplex tradeoff performance. This paper investigates and analyzes the QMF for the full-duplex (FD) relaying. Different from previous works, the relay has no access to any instantaneous channel state information (CSI), and only the statistical CSI of all channels is available. A closed-form expression for the outage probability is then derived. Due to the non-smoothness of the resulting expression, an approximate one with the smooth outage performance is further given. However, the resulting one is non-convex in general, and four suboptimal solutions of the quantizer design are derived. For comparison, the FD relaying with hybrid QMF/decode-and-forward is also studied. Besides, when the direct transmission (DT) is not available in both schemes, outage probability analysis and optimal quantizer design are also investigated. Simulation results demonstrate the correctness and tightness of the derived closed-form expressions for outage probabilities and close-to-optimal performance of the suboptimal quantizer design with DT.

INDEX TERMS Full-duplex, quantize-map-and-forward, hybrid quantize-map-and-forward/decode-and-forward.

I. INTRODUCTION

Cooperative communication has been recognized as an effective way to improve the performance of the direct transmission by the aid of single/multiple relays [1]. It has also demonstrated its successful applications in spectrum sensing [2], spectrum sharing [3], [4], physical-layer security [5], and energy harvesting [6], etc. For relaying strategies, amplify-and-forward (AF) and decode-and-forward (DF) are considered due to their simplicity and easy-to-implement. To further improve their performance, new strategies are proposed, see, e.g., opportunistic DF (ODF) [3], uncoded DF (UDF) [3], ODF/AF [4], and compress-and-forward (CF) [7]. Recently, quantize-map-and-forward (QMF) has been investigated and proved to achieved the capacity of arbitrary networks within a bounded additive gap, which is in contrast to traditional AF/DF relaying strategies [8]. It was also shown in [9] that QMF can significantly outperform CF, and achieve the optimal diversity-multiplexing tradeoff (DMT) at asymptotically high signal-to-noise ratio (SNR).

On the other hand, most of previous works focus on half-duplex relaying (see [9]–[13] and references therein), where

the relay cannot receive and forward simultaneously. Thus, more time slots are needed compared with the full-duplex relaying, and further decreasing the spectral efficiency. Note that in [14], half-duplex relays were used to implement the virtual full-duplex relaying. However, the full-duplex relaying with QMF has received few attention, which can be found in [8] and [15]. In [8], full/half duplex single/multiple relay networks were investigated with global/partial instantaneous channel state information (ICSI), where QMF, hybrid QMF/DF, DF and Dynamic DF (DDF) were considered for performance comparison. In [15], low density parity check code (LDPC) for encoding and relay map and message-passing algorithms for decoding were investigated for QMF, which has demonstrated its performance advantage over routing, opportunistic routing, AF and AF with beamforming.

In this paper, we analyze the outage probability and optimize the quantization level of the FD relaying with QMF and hybrid QMF/DF. Although [8] considered a similar system model, the analysis of the outage performance and the optimization of the quantization level are quite different. Specifically, the difference between [8] and this work is

two-fold. On one hand, for QMF, the global/partial ICSI at the relay was investigated for analysis and optimization. However, the resulting quantization levels are subject to channel estimation errors, and the outage performance with only the SCSI is still unknown. On the other hand, for hybrid QMF/DF, the outage performance was evaluated by the previously derived quantization level with ICSI. Thus, the problem of channel estimation errors and the SCSI performance as mentioned earlier in QMF also exists. Furthermore, the contribution of this work is summarized as follows:

- 1) Closed-form expressions for outage probabilities of the FD relaying with QMF and hybrid QMF/DF are derived, where there is no ICSI available at the relay. Approximate ones are introduced to deal with the non-smoothness of the outage performance. Outage probabilities of both schemes without direct transmission (DT) are also analyzed. Simulation results verify the correctness and tightness of the derived expressions.
- 2) Since the outage probability is generally non-convex over the quantization level, we turn to seek suboptimal solutions by minimizing its upper bound. Specifically, four special cases are considered for both QMF and hybrid QMF/DF, and corresponding optimal/suboptimal solutions are derived in four closed-form expressions. Unlike [8], the corresponding quantize levels depend on the rate threshold and/or channel statistics, instead of ICSI. Simulation results show that the suboptimal solutions to the quantizer design can achieve satisfactory performance, and the solution of the first case performs close to the numerically evaluated optimal solution to the original problem for both QMF and hybrid QMF/DF.
- 3) The optimal quantizer design for QMF without DT is considered, where the optimal solution is obtained for exact outage probability minimization. Hybrid QMF/DF without DT is, however, independent of the quantization level. Both analytical and simulations results show that the both schemes will suffer from a non-negligible performance loss in the absence of the DT.

The rest of this paper is organized as follows. Section II presents the system model and the transmission schemes for QMF and hybrid QMF/DF. Section III analyzes the outage probability, and Section IV and Section V give the suboptimal/optimal solutions to the quantizer design with/without DT, respectively. Section VI numerically evaluates the outage performance and performance comparison of optimal and suboptimal solutions, and Section VII concludes this paper.

II. SYSTEM MODEL

We consider a single relay network, in which there is one source S , one relay R and one destination D . Channel gains between S and R , R and D , S and D are respectively given by h_{SR} , h_{RD} and h_{SD} . Moreover, they are Rayleigh-faded with zero-mean and variances $E(|h_{SR}|^2)$, $E(|h_{RD}|^2)$ and $E(|h_{SD}|^2)$, respectively, and are independent of each other.

In this paper, it is assumed that S and R have the same transmit power, which is denoted as P . The additive white

Gaussian noise (AWGN) is with zero mean and variance δ^2 . Let $\bar{\gamma} = P/\delta^2$, then the channel power gain can be respectively expressed as $g_{SR} = \bar{\gamma}|h_{SR}|^2$, $g_{RD} = \bar{\gamma}|h_{RD}|^2$ and $g_{SD} = \bar{\gamma}|h_{SD}|^2$.

A. QMF

In this scheme, R quantizes the received signal with distortion Δ using the Gaussian vector quantizers, maps the quantized one into a codebook, and finally forwards the new codeword to D . The achievable rate of this scheme is given by [8]

$$R_{QMF} = \max\left(0, \min\left(\ln\left(1 + \frac{g_{SR}}{1 + \Delta} + g_{SD}\right), \ln\left(1 + g_{RD} + g_{SD}\right) - \ln\left(1 + \frac{1}{\Delta}\right)\right)\right), \quad (1)$$

where $\ln(\cdot)$ denotes the natural logarithm, and Δ is the quantization level.

B. HYBRID QMF/DF

In this scheme, R switches between the QMF and the DF modes depending on the decoding at R . If R can successfully decode the received signal, then it will re-encode the decoding one and forward the new one to D . Otherwise, R will quantize and map the received signal and forward it to D . The achievable rate of this scheme is given by [8]

$$R_{HQMF/DF} = \begin{cases} \ln(1 + g_{RD} + g_{SD}), & \ln(1 + g_{SR}) \geq R_{th} \\ R_{QMF}, & \ln(1 + g_{SR}) < R_{th} \end{cases} \quad (2)$$

where R_{th} denotes the rate threshold.

III. OUTAGE PROBABILITY ANALYSIS

In this section, we investigate and analyze the outage probability of both QMF and hybrid QMF/DF. Note that, in [8], the outage performance for QMF was examined in the following three cases depending on the availability of ICSI at R : 1) available ICSI of g_{SR} , g_{RD} and g_{SD} ; 2) available ICSI of g_{SR} , g_{RD} and SCSI of g_{SD} ; 3) available ICSI of g_{SR} , and SCSI of g_{RD} and g_{SD} . Besides, the outage performance of hybrid QMF/DF was examined numerically, in which Δ depends on the ICSI. Different from [8], we derive closed-expressions for outage probabilities in both schemes by taking only SCSI of g_{SR} , g_{RD} and g_{SD} into consideration, in which Δ is treated as a constant and will be optimized in the next section.

A. QMF

In this scheme, the outage happens when the achievable rate is less than R_{th} , and the outage probability $Pr\{R_{QMF} < R_{th}\}$ is given in (5)–(8). Moreover, exact closed-form expressions of I_2 and I_3 are shown in (35)–(38) in the Appendix.

However, in I_2 and I_3 , I_2' and I_3' are expressed as piecewise functions, in which their values depend on $\frac{1}{\lambda_{SD}}$ and $\frac{1+\Delta}{\lambda_{SR}} + \frac{1}{\lambda_{RD}}$, and $\frac{1}{\lambda_{SD}}$ and $\frac{1}{\lambda_{RD}}$, respectively. This results in the non-smoothness of the outage probability. By introducing a small

constant ϵ to I'_2 and I'_3 , approximate closed-form expressions are given by transforming the discrete values into continuous ones, which are shown in (12)–(13) at the top of the next page.

In summary, in QMF, based on the exact expressions in I_4 and approximate expressions in I'_2 and I'_3 , we have

$$P_{out}^{QMF} \approx 1 - I_2 - I_3 - I_4. \quad (3)$$

Moreover, when the direct transmission between S and D is not available, i.e., $g_{SD} = 0$, the outage probability in QMF is given by

$$\begin{aligned} P_{out,noDT}^{QMF} &= 1 - Pr \left\{ \ln \left(1 + \frac{g_{SR}}{1 + \Delta_{noDT}} \right) \geq R_{th}, \right. \\ &\quad \left. \ln \left(1 + g_{RD} \right) - \ln \left(1 + \frac{1}{\Delta_{noDT}} \right) \geq R_{th} \right\} \\ &= 1 - \exp \left(- \frac{(1 + \Delta_{noDT})(\exp(R_{th}) - 1)}{\lambda_{SR}} \right. \\ &\quad \left. - \frac{\left(1 + \frac{1}{\Delta_{noDT}} \right) \exp(R_{th}) - 1}{\lambda_{RD}} \right), \end{aligned} \quad (4)$$

where the derivations are similar to (3), and thus omitted for brevity. It can be easily verified that $P_{out,noDT}^{QMF} \geq P_{out}^{QMF}$.

B. HYBRID QMF/DF

In this scheme, the outage happens when the system cannot support R_{th} either in the DF or the QMF mode for successful and unsuccessful decoding, respectively. Specifically, the outage probability $Pr\{R_{HQMF/DF} < R_{th}\}$ is given on (14)–(18). Moreover, exact closed-form expressions of I_6 , I_9 and I_{10} given in (39)–(45).

However, hybrid QMF/DF inherits the problem of non-smoothness of the outage probability as in QMF. To see this, $I'_{9,1}$ depends on $\frac{1}{\lambda_{SD}}$ and $\frac{1+\Delta}{\lambda_{SR}} + \frac{1}{\lambda_{RD}}$, and I'_6 , $I'_{9,2}$ and I'_{10} depend on $\frac{1}{\lambda_{SD}}$ and $\frac{1}{\lambda_{RD}}$. Similar to the QMF, we adopt the same smooth method by introducing ϵ to I'_6 , $I'_{9,1}$, $I'_{9,2}$ and I'_{10} , respectively, which are shown in (20)–(23).

In summary, in hybrid QMF/DF, based on exact expressions in I_7 and I_{11} and approximate expressions in I'_6 , $I'_{9,1}$, $I'_{9,2}$ and I'_{10} , we have

$$P_{out}^{HQMF/DF} \approx I_6 + I_7 - I_9 - I_{10} - I_{11}. \quad (9)$$

Moreover, when the direct transmission between S and D is not available, i.e., $g_{SD} = 0$, the outage probability in hybrid QMF/DF is given by

$$\begin{aligned} P_{out,noDT}^{HQMF/DF} &= Pr \{ \ln(1 + g_{RD}) < R_{th} \} Pr \{ \ln(1 + g_{SR}) \geq R_{th} \} \\ &\quad + Pr \{ \ln(1 + g_{SR}) < R_{th} \} \\ &= 1 - \exp \left(- \left(\frac{1}{\lambda_{SR}} + \frac{1}{\lambda_{RD}} \right) (\exp(R_{th}) - 1) \right). \end{aligned} \quad (10)$$

It is interesting to point out that (10) is independent of Δ , and we also have $P_{out,noDT}^{HQMF/DF} \geq P_{out}^{HQMF/DF}$.

IV. SUBOPTIMAL QUANTIZER DESIGN WITH DT

The previous section has derived approximations for outage probabilities in both schemes, which are, however, non-convex over Δ . Thus, it is difficult to get the optimal Δ for outage minimization. In this section, we derive four suboptimal solutions for the quantizer design, in which the upper bound on the outage probability is minimized. For simplicity of analysis, we first consider QMF, and then extend it to hybrid QMF/DF.

A. QMF

Let us consider the following four cases by comparing g_{SR} and g_{SD} , and g_{RD} and g_{SD} in I_1 , respectively.

1) If $g_{SR} \geq g_{SD}$ and $g_{RD} \geq g_{SD}$, I_1 can be lower bounded by $I_{1,LB}^1$, which is shown in (24). Thus, the minimization of P_{out}^{QMF} is reduced to the maximization of $I_{1,LB}^1$.

$$\begin{aligned} P_{out}^{QMF} &= Pr \left\{ \min \left(\ln \left(1 + \frac{g_{SR}}{1 + \Delta} + g_{SD} \right), \ln(1 + g_{RD} + g_{SD}) - \ln \left(1 + \frac{1}{\Delta} \right) \right) < R_{th}, \ln(1 + g_{RD} + g_{SD}) > \ln \left(1 + \frac{1}{\Delta} \right) \right\} \\ &\quad + Pr \left\{ \ln(1 + g_{RD} + g_{SD}) \leq \ln \left(1 + \frac{1}{\Delta} \right) \right\} \\ &= 1 - Pr \left\{ \underbrace{\ln \left(1 + \frac{g_{SR}}{1 + \Delta} + g_{SD} \right) \geq R_{th}, \ln(1 + g_{RD} + g_{SD}) - \ln \left(1 + \frac{1}{\Delta} \right) \geq R_{th}}_{I_1=I_2+I_3+I_4} \right\} \end{aligned} \quad (5)$$

$$I_2 = Pr \left\{ g_{SR} \geq (1 + \Delta)(\exp(R_{th}) - 1 - g_{SD}), g_{RD} \geq \left(1 + \frac{1}{\Delta} \right) \exp(R_{th}) - 1 - g_{SD}, g_{SD} < \exp(R_{th}) - 1 \right\} \quad (6)$$

$$I_3 = Pr \left\{ g_{RD} \geq \left(1 + \frac{1}{\Delta} \right) \exp(R_{th}) - 1 - g_{SD}, \exp(R_{th}) - 1 \leq g_{SD} < \left(1 + \frac{1}{\Delta} \right) \exp(R_{th}) - 1 \right\} \quad (7)$$

$$I_4 = Pr \left\{ g_{SD} \geq \left(1 + \frac{1}{\Delta} \right) \exp(R_{th}) - 1 \right\} = \exp \left(- \frac{\left(1 + \frac{1}{\Delta} \right) \exp(R_{th}) - 1}{\lambda_{SD}} \right) \quad (8)$$

$$I'_2 \approx \frac{1}{\frac{1}{\lambda_{SD}} - \frac{1+\Delta}{\lambda_{SR}} - \frac{1}{\lambda_{RD}} + \epsilon} \left(1 - \exp \left(- \left(\frac{1}{\lambda_{SD}} - \frac{1+\Delta}{\lambda_{SR}} - \frac{1}{\lambda_{RD}} + \epsilon \right) (\exp(R_{th}) - 1) \right) \right) \quad (12)$$

$$I'_3 \approx \frac{1}{\frac{1}{\lambda_{SD}} - \frac{1}{\lambda_{RD}} + \epsilon} \exp \left(- \left(\frac{1}{\lambda_{SD}} - \frac{1}{\lambda_{RD}} + \epsilon \right) (\exp(R_{th}) - 1) \right) \left(1 - \exp \left(- \left(\frac{1}{\lambda_{SD}} - \frac{1}{\lambda_{RD}} + \epsilon \right) \frac{\exp(R_{th})}{\Delta} \right) \right) \quad (13)$$

$$P_{out}^{HQMF/DF} = \underbrace{\Pr \left\{ \max \left(0, \min \left(\ln \left(1 + \frac{g_{SR}}{1+\Delta} + g_{SD} \right), \ln(1 + g_{RD} + g_{SD}) - \ln \left(1 + \frac{1}{\Delta} \right) \right) \right) < R_{th}, \ln(1 + g_{SR}) < R_{th} \right\}}_{I_5} + \underbrace{\Pr \{ \ln(1 + g_{RD} + g_{SD}) < R_{th} \} \Pr \{ \ln(1 + g_{SR}) \geq R_{th} \}}_{I_6} \quad (14)$$

$$I_5 = \underbrace{\Pr \{ \ln(1 + g_{SR}) < R_{th} \}}_{I_7=1-\exp\left(-\frac{\exp(R_{th})-1}{\lambda_{SR}}\right)} - \underbrace{\Pr \left\{ \ln \left(1 + \frac{g_{SR}}{1+\Delta} + g_{SD} \right) \geq R_{th}, \ln(1 + g_{RD} + g_{SD}) - \ln \left(1 + \frac{1}{\Delta} \right) \geq R_{th}, \ln(1 + g_{SR}) < R_{th} \right\}}_{I_8=I_9+I_{10}+I_{11}} \quad (15)$$

$$I_9 = \Pr \left\{ (1 + \Delta)(\exp(R_{th}) - 1 - g_{SD}) \leq g_{SR} < \exp(R_{th}) - 1, g_{RD} \geq \left(1 + \frac{1}{\Delta} \right) \exp(R_{th}) - 1 - g_{SD}, \right. \\ \left. \times \frac{\Delta}{1 + \Delta} (\exp(R_{th}) - 1) < g_{SD} < \exp(R_{th}) - 1 \right\} \quad (16)$$

$$I_{10} = \Pr \{ g_{SR} < \exp(R_{th}) - 1 \} \Pr \left\{ g_{RD} \geq \left(1 + \frac{1}{\Delta} \right) \exp(R_{th}) - 1 - g_{SD}, \exp(R_{th}) - 1 \leq g_{SD} < \left(1 + \frac{1}{\Delta} \right) \exp(R_{th}) - 1 \right\} \quad (17)$$

$$I_{11} = \Pr \{ g_{SR} < \exp(R_{th}) - 1 \} \Pr \left\{ g_{SD} \geq \left(1 + \frac{1}{\Delta} \right) \exp(R_{th}) - 1 \right\} \\ = \left(1 - \exp \left(- \frac{\exp(R_{th}) - 1}{\lambda_{SR}} \right) \right) \exp \left(- \frac{\left(1 + \frac{1}{\Delta} \right) \exp(R_{th}) - 1}{\lambda_{SD}} \right) \quad (18)$$

Proposition 1: The optimal solution to maximize $I_{1,LB}^1$ is given by

$$\Delta_1^* = \frac{\exp(R_{th}) + \sqrt{9\exp(2R_{th}) - 8\exp(R_{th})}}{2(\exp(R_{th}) - 1)}. \quad (11)$$

Proof: If $\Delta_1 \leq \Delta_1^*$, then we have

$$I_{1,LB}^1 = \exp \left(- \frac{1}{2\lambda_{SD}} \left(\left(1 + \frac{1}{\Delta_1} \right) \exp(R_{th}) - 1 \right) \right).$$

Otherwise, we have

$$I_{1,LB}^1 = \exp \left(- \frac{1}{\lambda_{SD} \left(1 + \frac{1}{1+\Delta_1} \right)} (\exp(R_{th}) - 1) \right).$$

It can be easily checked that $I_{1,LB}^1$ is an increasing function in $(0, \Delta_1^*]$, and a decreasing function in $[\Delta_1^*, \infty)$. Thus, $I_{1,LB}^1$ is a quasi-concave function, which has its maximum at Δ_1^* . This completes the proof.

Proposition 1 indicates Δ_1^* depends only on R_{th} that is easy to get in practice, and there is no need to obtain $\lambda_{SR}, \lambda_{RD}$

and λ_{SD} . This is simply due to the assumption made in this case.

2) If $g_{SR} \geq g_{SD}$ and $g_{RD} < g_{SD}$, I_1 can be lower bounded by $I_{1,LB}^2$, which is shown in (25).

Similar to the first case, we can arrive at the following optimization problem

$$\min_{\Delta_2} \frac{\exp(R_{th}) - 1}{\left(1 + \frac{1}{1+\Delta_2} \right) \lambda_{SD}} + \frac{\left(1 + \frac{1}{\Delta_2} \right) \exp(R_{th}) - 1}{2\lambda_{RD}} \\ \text{s.t. } \Delta_2 > 0 \quad (19)$$

However, (19) is generally nonconvex. A suboptimal solution is summarized in the following proposition.

Proposition 2: The suboptimal solution to maximize $I_{1,LB}^2$ is given by

$$\Delta_2^* = \sqrt{\frac{\exp(R_{th})\lambda_{SD}}{2(\exp(R_{th}) - 1)\lambda_{RD}}}. \quad (28)$$

$$I'_6 = \frac{1}{\frac{1}{\lambda_{SD}} - \frac{1}{\lambda_{RD}} + \epsilon} \left(1 - \exp \left(- \left(\frac{1}{\lambda_{SD}} - \frac{1}{\lambda_{RD}} + \epsilon \right) (\exp(R_{th}) - 1) \right) \right) \quad (20)$$

$$I'_{9,1} \approx \frac{1}{\frac{1}{\lambda_{SD}} - \frac{1+\Delta}{\lambda_{SR}} - \frac{1}{\lambda_{RD}} + \epsilon} \exp \left(- \left(\frac{1}{\lambda_{SD}} - \frac{1+\Delta}{\lambda_{SR}} - \frac{1}{\lambda_{RD}} + \epsilon \right) \frac{\Delta(\exp(R_{th}) - 1)}{1 + \Delta} \right) \times \left(1 - \exp \left(- \left(\frac{1}{\lambda_{SD}} - \frac{1+\Delta}{\lambda_{SR}} - \frac{1}{\lambda_{RD}} + \epsilon \right) \frac{(\exp(R_{th}) - 1)}{1 + \Delta} \right) \right) \quad (21)$$

$$I'_{9,2} \approx \frac{1}{\frac{1}{\lambda_{SD}} - \frac{1}{\lambda_{RD}} + \epsilon} \exp \left(- \left(\frac{1}{\lambda_{SD}} - \frac{1}{\lambda_{RD}} + \epsilon \right) \frac{\Delta(\exp(R_{th}) - 1)}{1 + \Delta} \right) \left(1 - \exp \left(- \left(\frac{1}{\lambda_{SD}} - \frac{1}{\lambda_{RD}} + \epsilon \right) \frac{(\exp(R_{th}) - 1)}{1 + \Delta} \right) \right) \quad (22)$$

$$I'_{10} \approx \frac{1}{\frac{1}{\lambda_{SD}} - \frac{1}{\lambda_{RD}} + \epsilon} \exp \left(- \left(\frac{1}{\lambda_{SD}} - \frac{1}{\lambda_{RD}} + \epsilon \right) (\exp(R_{th}) - 1) \right) \left(1 - \exp \left(- \left(\frac{1}{\lambda_{SD}} - \frac{1}{\lambda_{RD}} + \epsilon \right) \frac{\exp(R_{th})}{\Delta} \right) \right) \quad (23)$$

$$I_1 \geq \underbrace{Pr \left\{ \ln \left(1 + \left(1 + \frac{1}{1 + \Delta_1} \right) g_{SD} \right) \geq R_{th}, \ln(1 + 2g_{SD}) - \ln \left(1 + \frac{1}{\Delta_1} \right) \geq R_{th} \right\}}_{I_{1,LB}^1} \\ = \exp \left(- \frac{1}{\lambda_{SD}} \max \left(\frac{1}{\left(1 + \frac{1}{1 + \Delta_1} \right)} (\exp(R_{th}) - 1), \frac{1}{2} \left(\left(1 + \frac{1}{\Delta_1} \right) \exp(R_{th}) - 1 \right) \right) \right) \quad (24)$$

$$I_1 \geq \underbrace{Pr \left\{ \ln \left(1 + \left(1 + \frac{1}{1 + \Delta_2} \right) g_{SD} \right) \geq R_{th}, \ln(1 + 2g_{RD}) - \ln \left(1 + \frac{1}{\Delta_2} \right) \geq R_{th} \right\}}_{I_{1,LB}^2} \\ = \exp \left(- \frac{\exp(R_{th}) - 1}{\left(1 + \frac{1}{1 + \Delta_2} \right) \lambda_{SD}} - \frac{\left(1 + \frac{1}{\Delta_2} \right) \exp(R_{th}) - 1}{2\lambda_{RD}} \right) \quad (25)$$

$$I_1 \geq \underbrace{Pr \left\{ \ln \left(1 + \left(1 + \frac{1}{1 + \Delta_3} \right) g_{SR} \right) \geq R_{th}, \ln(1 + 2g_{SD}) - \ln \left(1 + \frac{1}{\Delta_3} \right) \geq R_{th} \right\}}_{I_{1,LB}^3} \\ = \exp \left(- \frac{\exp(R_{th}) - 1}{\left(1 + \frac{1}{1 + \Delta_3} \right) \lambda_{SR}} - \frac{\left(1 + \frac{1}{\Delta_3} \right) \exp(R_{th}) - 1}{2\lambda_{SD}} \right) \quad (26)$$

$$I_1 \geq \underbrace{Pr \left\{ \ln \left(1 + \left(1 + \frac{1}{1 + \Delta_4} \right) g_{SR} \right) \geq R_{th}, \ln(1 + 2g_{RD}) - \ln \left(1 + \frac{1}{\Delta_4} \right) \geq R_{th} \right\}}_{I_{1,LB}^4} \\ = \exp \left(- \frac{\exp(R_{th}) - 1}{\left(1 + \frac{1}{1 + \Delta_4} \right) \lambda_{SR}} - \frac{\left(1 + \frac{1}{\Delta_4} \right) \exp(R_{th}) - 1}{2\lambda_{RD}} \right) \quad (27)$$

Proof: After some manipulations of $I_{1,LB}^2$, we have the following optimization problem

$$\min_{\Delta_2} \frac{(\exp(R_{th}) - 1)\Delta_2}{\lambda_{SD}} + \frac{\exp(R_{th})}{2\lambda_{RD}\Delta_2}, \text{ s.t. } \Delta_2 > 0. \quad (29)$$

It can be easily verified that (29) is a convex function over Δ , and the optimal solution is given by taking its first derivative and setting it equal to zero. This completes the proof.

Proposition 2 indicates Δ_2^* requires not only R_{th} but also additional information of the ratio of λ_{SD} to λ_{RD} if compared with proposition 1.

3) If $g_{SR} < g_{SD}$ and $g_{RD} \geq g_{SD}$, I_1 can be lower bounded by $I_{1,LB}^3$, which is shown in (26). Similar to the second case, its optimal solution is given by

$$\Delta_3^* = \sqrt{\frac{\exp(R_{th})\lambda_{SR}}{2(\exp(R_{th}) - 1)\lambda_{SD}}}. \quad (30)$$

4) If $g_{SR} < g_{SD}$ and $g_{RD} < g_{SD}$, I_1 can be lower bounded by $I_{1,LB}^4$, which is shown in (27). Similar to the second case, its optimal solution is

given by

$$\Delta_4^* = \sqrt{\frac{\exp(R_{th})\lambda_{SR}}{2(\exp(R_{th}) - 1)\lambda_{RD}}}. \quad (31)$$

B. HYBRID QMF/DF

Note that I_5 in the $P_{out}^{HQMF/DF}$ is upper bounded by P_{out}^{QMF} , which means that (11), (29), (30) and (31) can be applied to $P_{out}^{HQMF/DF}$ for its upper bound minimization. That is to say, (11), (29), (30) and (31) are unifying suboptimal solutions for the quantizer design for both schemes.

Before leaving this section, it is desirable to point out derived closed-form expressions for suboptimal solutions depends only on R_{th} and/or SCSI of g_{SR} , g_{RD} and g_{SD} . This is in contrast to [8], where Δ^* depends on the global/partial ICSI, and thus is subject to channel estimation errors.

V. OPTIMAL QUANTIZER DESIGN WITHOUT DT

Recall that $P_{out,noDT}^{HQMF/DF}$ in (10) is independent of Δ , we focus on the minimization of $P_{out,noDT}^{QMF}$ in (4) with respect to Δ_{noDT} , which is given by

$$\min_{\Delta_{noDT}} \frac{(\exp(R_{th}) - 1)\Delta_{noDT}}{\lambda_{SR}} + \frac{\exp(R_{th})}{\lambda_{RD}\Delta_{noDT}}, \quad \text{s.t. } \Delta_{noDT} > 0. \quad (32)$$

Similar to the second case in the previous Section, the optimal solution is given by

$$\Delta_{noDT}^* = \sqrt{\frac{\exp(R_{th})\lambda_{SR}}{(\exp(R_{th}) - 1)\lambda_{RD}}}. \quad (33)$$

By substituting (32) into (4), the optimal $P_{out,noDT}^{QMF}$ is given by

$$P_{out,noDT}^{QMF} = 1 - \exp\left(-\left(\frac{1}{\lambda_{SR}} + \frac{1}{\lambda_{RD}}\right)(\exp(R_{th}) - 1)\right) \times \exp\left(-\sqrt{\frac{\exp(R_{th})(\exp(R_{th}) - 1)}{\lambda_{SR}\lambda_{RD}}}\right). \quad (34)$$

Therefore, it can be easily verified that $P_{out,noDT}^{QMF}$ in (34) is no less than $P_{out,noDT}^{HQMF/DF}$ in (10).

VI. NUMERICAL RESULTS

In this section, we numerically investigate and analyze the outage probability and the quantizer design for both QMF and hybrid QMF/DF with/without DT. Recall that, in [8], various comparison with traditional DF and dynamic DF was given, and QMF and hybrid QMF/DF were shown their performance superiority. Thus, we will focus on the performance of both schemes in this section. In our simulations, both independent and identically distributed (i.i.d.) and independent and non-identically distributed (i.n.i.d.) channels are considered. To be specific, in i.i.d. channels, we have $E(|h_{SR}|^2) = E(|h_{RD}|^2) = E(|h_{SD}|^2) = 1$, while in i.n.i.d. channels, we have $E(|h_{SR}|^2) = E(|h_{RD}|^2) = 1$ and $E(|h_{SD}|^2) = 0.1$.

Besides, $R_{th} = 2 \text{ nats/s/Hz}$ and $\epsilon = 10^{-6}$ are set. However, our contributions are not limited to the these parameter settings.

A. OUTAGE PROBABILITY ANALYSIS

First, we evaluate the analytical results in (3) and (9) for QMF and hybrid QMF/DF. For comparison, simulation results are provided by averaging 10^6 independent runs.

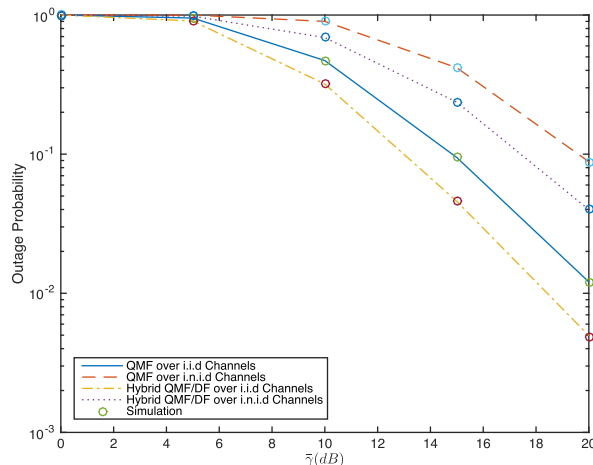


FIGURE 1. Outage performance comparison of QMF and hybrid QMF/DF with $\Delta = 1$.

Fig. 1 shows the outage probability versus $\bar{\gamma}$ for both schemes. It is found that there is a precise agreement between our analytical and simulation results, which can validate the correctness of (3) and (9). Moreover, it is also observed that hybrid QMF/DF outperforms QMF, which is consistent with analytical and simulations results in [8] with global/partial ICSI. Besides, the performance of both schemes deteriorates dramatically in i.n.i.d. channels compared with that in i.i.d. ones, which is simply due to the low $E(|h_{SD}|^2)$.

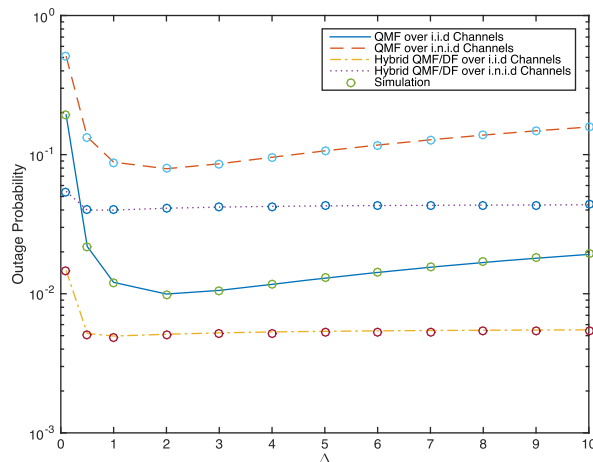


FIGURE 2. Outage performance comparison of QMF and hybrid QMF/DF with $\bar{\gamma} = 20 \text{ dB}$.

Fig. 2 shows the outage probability versus Δ for both schemes. Recall that I_2' in P_{out}^{QMF} and $I_{0,1}'$ in $P_{out}^{HQMF/DF}$ are

$$I_2 = \exp \left(\frac{(1+\Delta)(\exp(R_{th}) - 1)}{\lambda_{SR}} - \frac{(1+\frac{1}{\Delta}) \exp(R_{th}) - 1}{\lambda_{RD}} \right) \frac{1}{\lambda_{SD}} \underbrace{\int_0^{\exp(R_{th})-1} \exp \left(- \left(\frac{1}{\lambda_{SD}} - \frac{1+\Delta}{\lambda_{SR}} - \frac{1}{\lambda_{RD}} \right) g_{SD} \right) dg_{SD}}_{I'_2} \quad (35)$$

$$I'_2 = \begin{cases} \frac{1}{\frac{1}{\lambda_{SD}} - \frac{1+\Delta}{\lambda_{SR}} - \frac{1}{\lambda_{RD}}} \left(1 - \exp \left(- \left(\frac{1}{\lambda_{SD}} - \frac{1+\Delta}{\lambda_{SR}} - \frac{1}{\lambda_{RD}} \right) (\exp(R_{th}) - 1) \right) \right), & \frac{1}{\lambda_{SD}} \neq \frac{1+\Delta}{\lambda_{SR}} + \frac{1}{\lambda_{RD}} \\ \exp(R_{th}) - 1, & \text{otherwise} \end{cases} \quad (36)$$

$$I_3 = \exp \left(- \frac{(1+\frac{1}{\Delta}) \exp(R_{th}) - 1}{\lambda_{RD}} \right) \frac{1}{\lambda_{SD}} \underbrace{\int_{\exp(R_{th})-1}^{(1+\frac{1}{\Delta}) \exp(R_{th})-1} \exp \left(- \left(\frac{1}{\lambda_{SD}} - \frac{1}{\lambda_{RD}} \right) g_{SD} \right) dg_{SD}}_{I'_3} \quad (37)$$

$$I'_3 = \begin{cases} \frac{1}{\frac{1}{\lambda_{SD}} - \frac{1}{\lambda_{RD}}} \exp \left(- \left(\frac{1}{\lambda_{SD}} - \frac{1}{\lambda_{RD}} \right) (\exp(R_{th}) - 1) \right) \left(1 - \exp \left(- \left(\frac{1}{\lambda_{SD}} - \frac{1}{\lambda_{RD}} \right) \frac{\exp(R_{th})}{\Delta} \right) \right), & \frac{1}{\lambda_{SD}} \neq \frac{1}{\lambda_{RD}} \\ \frac{\exp(R_{th})}{\Delta}, & \text{otherwise} \end{cases} \quad (38)$$

$$I_6 = \left(1 - \exp \left(- \frac{\exp(R_{th}) - 1}{\lambda_{SD}} \right) - \exp \left(- \frac{\exp(R_{th}) - 1}{\lambda_{RD}} \right) \right) \frac{1}{\lambda_{SD}} \underbrace{\int_0^{\exp(R_{th})-1} \exp \left(- \left(\frac{1}{\lambda_{SD}} - \frac{1}{\lambda_{RD}} \right) g_{SD} \right) dg_{SD}}_{I'_6} \times \exp \left(- \frac{\exp(R_{th}) - 1}{\lambda_{SR}} \right) \quad (39)$$

$$I'_6 = \begin{cases} \frac{1}{\frac{1}{\lambda_{SD}} - \frac{1}{\lambda_{RD}}} \left(1 - \exp \left(- \left(\frac{1}{\lambda_{SD}} - \frac{1}{\lambda_{RD}} \right) (\exp(R_{th}) - 1) \right) \right), & \frac{1}{\lambda_{SD}} \neq \frac{1}{\lambda_{RD}} \\ \exp(R_{th}) - 1, & \text{otherwise} \end{cases} \quad (40)$$

$$I_9 = \exp \left(\frac{(1+\Delta)(\exp(R_{th}) - 1)}{\lambda_{SR}} - \frac{(1+\frac{1}{\Delta}) \exp(R_{th}) - 1}{\lambda_{RD}} \right) \frac{1}{\lambda_{SD}} \underbrace{\int_{\frac{\Delta}{1+\Delta}(\exp(R_{th})-1)}^{\exp(R_{th})-1} \exp \left(- \left(\frac{1}{\lambda_{SD}} - \frac{1+\Delta}{\lambda_{SR}} - \frac{1}{\lambda_{RD}} \right) g_{SD} \right) dg_{SD}}_{I'_{9,1}} - \exp \left(\frac{\exp(R_{th}) - 1}{\lambda_{SR}} - \frac{(1+\frac{1}{\Delta}) \exp(R_{th}) - 1}{\lambda_{RD}} \right) \frac{1}{\lambda_{SD}} \underbrace{\int_{\frac{\Delta}{1+\Delta}(\exp(R_{th})-1)}^{\exp(R_{th})-1} \exp \left(- \left(\frac{1}{\lambda_{SD}} - \frac{1}{\lambda_{RD}} \right) g_{SD} \right) dg_{SD}}_{I'_{9,2}} \quad (41)$$

$$I'_{9,1} = \begin{cases} \frac{1}{\frac{1}{\lambda_{SD}} - \frac{1+\Delta}{\lambda_{SR}} - \frac{1}{\lambda_{RD}}} \exp \left(- \left(\frac{1}{\lambda_{SD}} - \frac{1+\Delta}{\lambda_{SR}} - \frac{1}{\lambda_{RD}} \right) \frac{\Delta}{1+\Delta} (\exp(R_{th}) - 1) \right) \times \left(1 - \exp \left(- \left(\frac{1}{\lambda_{SD}} - \frac{1+\Delta}{\lambda_{SR}} - \frac{1}{\lambda_{RD}} \right) \frac{\exp(R_{th}) - 1}{1+\Delta} \right) \right), & \frac{1}{\lambda_{SD}} \neq \frac{1+\Delta}{\lambda_{SR}} + \frac{1}{\lambda_{RD}} \\ \frac{\exp(R_{th}) - 1}{1+\Delta}, & \text{otherwise} \end{cases} \quad (42)$$

$$I'_{9,2} = \begin{cases} \frac{1}{\frac{1}{\lambda_{SD}} - \frac{1}{\lambda_{RD}}} \exp \left(- \left(\frac{1}{\lambda_{SD}} - \frac{1}{\lambda_{RD}} \right) \frac{\Delta}{1+\Delta} (\exp(R_{th}) - 1) \right) \left(1 - \exp \left(- \left(\frac{1}{\lambda_{SD}} - \frac{1}{\lambda_{RD}} \right) \frac{\exp(R_{th}) - 1}{1+\Delta} \right) \right), & \frac{1}{\lambda_{SD}} \neq \frac{1}{\lambda_{RD}} \\ \frac{\exp(R_{th}) - 1}{1+\Delta}, & \text{otherwise} \end{cases} \quad (43)$$

$$I_{10} = \left(1 - \exp \left(- \frac{\exp(R_{th}) - 1}{\lambda_{SR}} \right) \right) \exp \left(- \frac{(1+\frac{1}{\Delta}) \exp(R_{th}) - 1}{\lambda_{RD}} \right) \frac{1}{\lambda_{SD}} \underbrace{\int_{\exp(R_{th})-1}^{(1+\frac{1}{\Delta}) \exp(R_{th})-1} \exp \left(- \left(\frac{1}{\lambda_{SD}} - \frac{1}{\lambda_{RD}} \right) g_{SD} \right) dg_{SD}}_{I'_{10}} \quad (44)$$

$$I'_{10} = \begin{cases} \frac{1}{\frac{1}{\lambda_{SD}} - \frac{1}{\lambda_{RD}}} \exp \left(- \left(\frac{1}{\lambda_{SD}} - \frac{1}{\lambda_{RD}} \right) (\exp(R_{th}) - 1) \right) \left(1 - \exp \left(- \left(\frac{1}{\lambda_{SD}} - \frac{1}{\lambda_{RD}} \right) \frac{\exp(R_{th})}{\Delta} \right) \right), & \frac{1}{\lambda_{SD}} \neq \frac{1}{\lambda_{RD}} \\ \frac{\exp(R_{th})}{\Delta}, & \text{otherwise} \end{cases} \quad (45)$$

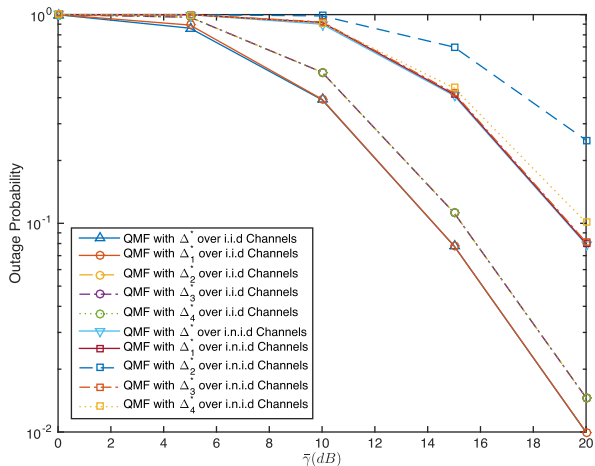


FIGURE 3. Suboptimal quantizer design for QMF with DT.

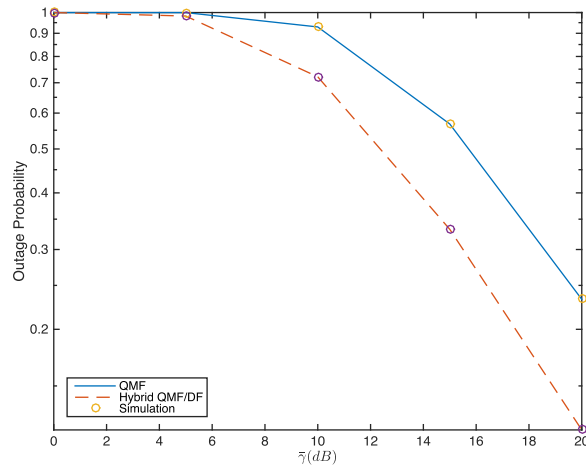


FIGURE 5. Optimal quantizer design for QMF without DT.

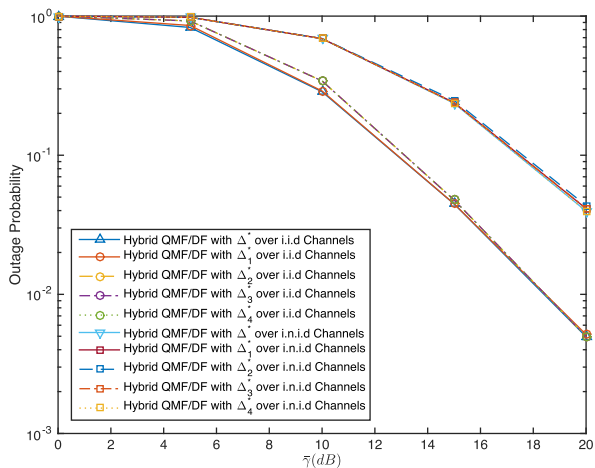


FIGURE 4. Suboptimal quantizer design for hybrid QMF/DF with DT.

piecewise functions of Δ . In i.n.i.d. channels, when $\Delta = 8$, we have $\frac{1}{\lambda_{SD}} = \frac{1+\Delta}{\lambda_{SR}} + \frac{1}{\lambda_{RD}}$, and I_2' and $I_{9,1}'$ will switch to different values. In this case, the performance will be non-smooth. However, due to the approximations in (3) and (9), there is no such case. This can verify the tightness of (3) and (9). On the other hand, in i.i.d. channels, it can be easily checked that the values of all piecewise functions for both schemes are fixed, and thus smooth. Besides, it is also seen that analytical results match well with simulation ones. Another observation is, although it is possible to search the minimum values for the outage performance in Fig. 2, it doesn't mean that (3) and (9) are always convex functions over Δ for any channel parameter setting.

B. SUBOPTIMAL QUANTIZER DESIGN WITH DT

Second, we evaluate the performance of suboptimal solutions, i.e., (11), (29), (30) and (31) for both schemes. For comparison, the optimal solutions are numerically given, which are searched over all possible values of outage probabilities for any given $\tilde{\gamma}$ and Δ considered in the simulation.

Fig. 3 shows the suboptimal quantizer design for QMF with DT. For i.i.d. channels, we have $\Delta_2^* = \Delta_3^* = \Delta_4^*$. This is why the corresponding outage performance is the same. For i.n.i.d. channels, the outage performance with Δ_2^* performs the worst. This can be verified in Fig. 2 where Δ_2^* is much less than 1. However, in all cases, there is almost no performance gap between curves by Δ^* and Δ_1^* . Recall that the optimal solutions is based on the exhaustive search, this indicates the outage performance with Δ_1^* is superior to those with Δ_2^* , Δ_3^* and Δ_4^* , and therefore chosen as the optimal one.

Fig. 4 shows the suboptimal quantizer design for hybrid QMF/DF with DT. Once again, it is also found the outage performance with Δ_1^* is almost identical to the optimal one. The outage performance with Δ_2^* , Δ_3^* and Δ_4^* are equal to each other in i.i.d. channels. However, it is seen that the performance difference among curves corresponding to four suboptimal solutions is negligible, which is contrast to Fig. 3. This is because, when the values of Δ_1^* , Δ_2^* , Δ_3^* and Δ_4^* are larger than 1, and their corresponding outage performance in hybrid QMF/DF is almost the same as illustrated in Fig. 2. Furthermore, in conclusions, it is desirable to adopt Δ_1^* for practical quantizer design due to its close-to-optimal outage performance for both schemes in i.i.d./i.n.i.d. channels as demonstrated in Fig. 3 and Fig. 4.

C. OPTIMAL QUANTIZER DESIGN WITHOUT DT

Last but not least, we evaluate the performance of optimal solutions for QMF in (34), where the comparison with hybrid QMF/DF in (10) is also considered. Fig. 5 shows the optimal quantizer design without DT for both schemes, where $E(|h_{SR}|^2) = E(|h_{RD}|^2) = 1$ and $E(|h_{SD}|^2) = 0$. As expected, the performance of both schemes deteriorates without the aid of DT, and hybrid QMF/DF performs better than QMF. Besides, it also reveals that both schemes benefit a lot from DT by a close comparison of Fig. 3, Fig. 4 and Fig. 5 with respect to the outage performance. Furthermore, analytical results in (4), (10), (33) and (34) can be also validated by simulation ones, due to the close match between them.

VII. CONCLUSION

This paper has analyzed the outage probability and optimized the quantizer of the FD relaying with both QMF and hybrid QMF/DF. For the outage probability analysis, exact closed-form expressions are derived for both schemes with/without DT, where the relay has only access to the SCS. In particular, the non-smoothness issue of exact closed-form expressions for both schemes in the presence of the DT is solved by approximate ones. Due to the generally non-convexity of the outage probability, the optimal quantizer design with the DT is not desirable, and four suboptimal solutions are proposed by minimizing its upper bound. Optimal quantizer design for QMF in the absence of the DT is further obtained. Simulation results have verified the correctness and tightness of the derived expressions. They also shown that the proposed suboptimal solutions can achieve satisfactory outage performance, particularly the one corresponding to the first case performs close to the numerically evaluated optimal one for both QMF and hybrid QMF/DF with DT.

APPENDIX

In the section, derivations of I_2 and I_3 for QMF and I_6 , I_9 and I_{10} for hybrid QMF/DF are given based on the fact that g_{SR} , g_{RD} and g_{SD} obey the exponential distribution with parameters $\lambda_{SR} = \bar{\gamma}E(|h_{SR}|^2)$, $\lambda_{RD} = \bar{\gamma}E(|h_{RD}|^2)$ and $\lambda_{SD} = \bar{\gamma}E(|h_{SD}|^2)$, respectively.

Since λ_{SR} , λ_{RD} and λ_{SD} are not necessarily the same, I'_2 , I'_3 , I'_6 , $I'_{9,1}$, $I'_{9,2}$ and I'_{10} should be expressed as piecewise functions. Thus, our derivations apply for not only i.i.d. but also i.n.i.d. channels. Details are given in (36), (38), (40), (42), (43), and (45).

REFERENCES

- [1] A. Nosratinia, T. E. Hunter, and A. Hedayat, "Cooperative communication in wireless networks," *IEEE Commun. Mag.*, vol. 42, no. 10, pp. 74–80, Oct. 2004.
- [2] Z. Quan, D. Li, and Y. Gong, "Cooperative signal classification using spectral correlation function in cognitive radio networks," in *Proc. IEEE Int. Conf. Commun. (ICC)*, May 2016, pp. 1–6.
- [3] D. Li, "Cognitive relay networks: Opportunistic or uncoded decode-and-forward relaying?" *IEEE Trans. Veh. Technol.*, vol. 63, no. 3, pp. 1486–1491, Mar. 2014.
- [4] D. Li, "Opportunistic DF-AF selection for cognitive relay networks," *IEEE Trans. Veh. Technol.*, vol. 65, no. 4, pp. 2790–2796, Apr. 2016.
- [5] L. Dong, Z. Han, A. P. Petropulu, and H. V. Poor, "Improving wireless physical layer security via cooperating relays," *IEEE Trans. Signal Process.*, vol. 58, no. 3, pp. 1875–1888, Mar. 2010.
- [6] K. Ishibashi, H. Ochiai, and V. Tarokh, "Energy harvesting cooperative communications," in *Proc. IEEE 23rd Int. Symp. Pers. Indoor Mobile Radio Commun. (PIMRC)*, Sep. 2012, pp. 1819–1823.
- [7] S. Yao and M. Skoglund, "Hybrid digital-analog relaying for cooperative transmission over slow fading channels," *IEEE Trans. Inf. Theory*, vol. 55, no. 3, pp. 944–951, Mar. 2009.
- [8] A. Sengupta, I.-H. Wang, and C. Fragouli, "Cooperative relaying at finite SNR—Role of quantize-map-and-forward," *IEEE Trans. Wireless Commun.*, vol. 13, no. 9, pp. 4857–4870, Sep. 2014.
- [9] S. Yao, T. T. Kim, M. Skoglund, and H. V. Poor, "Half-duplex relaying over slow fading channels based on quantize-and-forward," *IEEE Trans. Inf. Theory*, vol. 59, no. 2, pp. 860–872, Feb. 2013.
- [10] V. Nagpal, I. H. Wang, M. Jorgovanovic, D. Tse, and B. Nikolic, "Coding and system design for quantize-map-and-forward relaying," *IEEE J. Sel. Areas Commun.*, vol. 31, no. 8, pp. 1423–1435, Aug. 2013.
- [11] A. Ozgur and S. Diggavi, "Approximately achieving Gaussian relay network capacity with lattice-based QMF codes," *IEEE Trans. Inf. Theory*, vol. 59, no. 12, pp. 8275–8294, Dec. 2013.
- [12] R. Kolte, A. Özgür, and S. Diggavi, "When are dynamic relaying strategies necessary in half-duplex wireless networks?" *IEEE Trans. Inf. Theory*, vol. 61, no. 4, pp. 1720–1738, Apr. 2015.
- [13] F. Parvaresh and H. Soltanizadeh, "Diversity-multiplexing trade-off of half-duplex single relay networks," *IEEE Trans. Inf. Theory*, vol. 63, no. 3, pp. 1703–1720, Mar. 2017.
- [14] S.-N. Hong and G. Caire, "Virtual full-duplex relaying with half-duplex relays," *IEEE Trans. Inf. Theory*, vol. 61, no. 9, pp. 4700–4720, Sep. 2015.
- [15] A. Sengupta, S. Brahma, A. Ozgur, C. Fragouli, and S. Diggavi, "Graph-based codes for quantize-map-and-forward relaying," in *Proc. IEEE Inf. Theory Workshop (ITW)*, Oct. 2011, pp. 140–144.



DONG LI (M'10) received the B.E. degree in communication engineering from Yunnan University, Kunming, China, in 2004, and the M.E. and Ph.D. degrees in electronics and communication engineering from Sun Yat-sen University, Guangzhou, China, in 2006 and 2010, respectively. Since 2010, he has been with the Faculty of Information Technology, Macau University of Science and Technology (MUST), Macau, where he is currently an Associate Professor. He held research and visiting positions at the Institute for Infocomm Research, Singapore, and The Chinese University of Hong Kong, Shenzhen, China. His research interests include signal processing and machine learning for wireless communications, and Internet of Things. He was a recipient of the 2011 and 2016 MUST Bank of China Excellent Research Award. He served as a Technical Program Committee Vice Chair of the IEEE International Conference on Communications Systems in 2014.

...